17-dB Net Gain of Broadband Single-Mode Cr-Doped Crystalline Core Fiber Fabricated by Small Core

Chun-Nien Liu, Kai-Chieh Chang, Chia-Ling Tsai, Wei-Chih Cheng, Tien-Tsorng Shih, Sheng-Lung Huang, and Wood-Hi Cheng, *Life Fellow, IEEE*

***Abstract*—A record net gain of 17-dB has been demonstrated in a 300-nm broadband single-mode Cr-doped crystalline core fiber (CCF) with a 19-μm core diameter and 18-cm fiber length. The gain-per-unit-length of the CCF, which is an impressive 94 dB/m, is significantly higher than that currently achieved in other rare-earth doped fiber amplifiers, such as Er and Bi-doped fibers. This high gain was achieved by matching the transmission mode between CCF and single mode fiber for improving the coupling efficiency. We controlled precisely the conical molten-zone in the growth process, as well as the optimization of the Cr^{4+} concentration through thermal annealing and polarization pumping techniques. We also measured the noise figures of several core diameters, finding that the 19-μm core diameter CCF exhibited a noise figure 4.2 dB lower than the previous 25-μm core diameter CCF. This result is important because it indicates that the smaller diameter CCF is capable of providing even better signal-to-noise ratios. And the error-floor free data transmission of the CCF was successfully demonstrated at a rate of 10 Gb/s. This is an important achievement because it shows that the CCF has the potential to be used in high-speed communication applications.**

***Index Terms*—Fiber amplifier, annealing and polarization pump, net gain, and pump-to-signal-conversion-efficiency.**

I. Introduction

ERBIUM-DOPED fiber amplifier (EDFA) was one of the key optical communication technologies of the 20th century [1], [2], [3], [4]. Over the past 30 years, significant research and development efforts have been made to improve the EDFA, which has played a crucial role in the growth of the global optical communication market. However, the EDFA has limitations when it comes to bandwidth, as it can only be used for C- or L-band WDM transmission and utilizes just 45% of the low-loss transmission bandwidths from 1.3 to 1.6-μm in optical communication systems. While other fiber amplifiers, such as Tm-doped fiber (TDF) in the S-band [5], Pr-doped fiber (PDF) in the O-band [6], and Bi-doped fiber (BDF) in the U-band [7], have been developed, they cannot yet be used for a single fiber amplifier covering the entire 300-nm bandwidth. Recently, researchers have explored single-mode chromium-doped crystalline core fibers (CCFs) as possible candidates for broadband amplifiers to cover the interval from 1.3 to 1.6-μm [8], [9], [10]. The core of the CCF is composed of chromium doped with yttrium aluminum garnet (Cr:YAG), and the fluorescence spectrum of the CCF emitted from Cr^{3+}-ions of the octahedral site and Cr^{4+}-ions of the tetrahedral site provides a wide usable bandwidth. However, the high volatility of chromium oxide during the high-temperature growth process made it challenging to maintain a sufficient concentration of Cr^{4+}(tetra) -ions in the CCF. In a previous study, researchers reported on the fabrication of a 25-μm CCF and the dependence of gain on length and tetrahedral Cr^{4+}-ion concentration [11], [12]. However, the pump-to-signal-conversion efficiency (PSCE) of the CCF with a 25-μm core was less than 0.1%, making it impractical for use in broadband fiber amplifiers. This low PSCE was due to the low Cr^{4+}(tetra) concentration in the CCF core and the coupling mode-mismatch between the CCF and single-mode fiber.

Maintaining a high concentration of Cr^{4+}(tetra)-ions in the CCF core is difficult due to the volatility of chromium oxide during the high-temperature growth process. Previous research has shown that optimization of Cr^{4+}-ions in CCFs resulted in a net gain of 7.1-dB [9], 8.0-dB [10], 6.7-dB [11], and 11-dB [12]. To increase the fluorescence intensity of Cr:YAG, annealing of the Cr:YAG crystal can be performed to transform Cr^{3+}(octa)-ions into Cr^{4+}(tetra)-ions [8]. Further enhancement of the excited Cr^{4+}(tetra)-ions can be achieved by aligning the polarization of the pump and signal along the same crystal axis [12]. As for the coupling mode-mismatch between CCF and single-mode fiber, it is difficult to fabricate single-mode CCFs with small core diameters (<25 μm) and the small index difference cladding to achieve the V-number less than 2.405 [8].

Manuscript received 27 February 2023; revised 21 March 2023; accepted 26 March 2023. Date of publication 30 March 2023; date of current version 17 April 2023. This work was supported in part by the National Science and Technology Council, Taiwan under Grants 109-2221-E-005-075, 110-2222-E-005-003, 111-2221-E-005-024-MY2, and 111-2221-E-005-023-MY3, and in part by the Ministry of Education, Taiwan under Grant 111RA077A from Prof. Charles W. Tu. *(Corresponding author: Chun-Nien Liu.)*

Chun-Nien Liu is with the Department of Electrical Engineering, National Chung Hsing University, Taichung 402, Taiwan (e-mail: terbovine@gmail.com).

Kai-Chieh Chang and Sheng-Lung Huang are with the Graduate Institute of Photonics and Optoelectronics, National Taiwan University, Taipei 102, Taiwan (e-mail: chang3175@gmail.com; shuang@ntu.edu.tw).

Chia-Ling Tsai, Wei-Chih Cheng, and Wood-Hi Cheng are with the Graduates Institute of Optoelectronic Engineering, National Chung Hsing University, Taichung 402, Taiwan (e-mail: nikki1996210@gmail.com; weichih0428@gmail.com; whcheng@email.nchu.edu.tw).

Tien-Tsorng Shih is with the Department of Electronic Engineering, National Kaohsiung University of Applied Sciences, Kaohsiung 800, Taiwan (e-mail: tt@nkust.edu.tw).

Digital Object Identifier 10.1109/JPHOT.2023.3263126

TABLE I
COMPARISON OF NET GAIN FOR DIFFERENT DOPED FIBERS

Reference	Type	Net Gain (dB)	Gain-Per-Unit-Length (dB/m)	Core Dia. (μm)
2017 JLT [8]	CDF	6.4	27	25
2019 OFC [9]	CDF	7.1	30	25
2020 PJ [10]	CDF	8.0	30	25
2020 OFC [11]	CDF	6.7	34	25
2021 JLT [12]	CDF	11	32	25
This study	CDF	17	94	19

In this study, we improved the laser heated pedestal growth (LHPG) process by implementing a better control loop and more precise control to fabricate CCFs with a smaller core diameter and the high-index glass cladding. Compared to previous reports [8], [9], [11], [12], the obtained net gain of 17-dB is the highest value reported for CCFs (see Table I). The 19-μm core diameter fiber exhibits an average 2.2-dB lower noise figure than the larger 25-μm core. Optical data transmission at 10 Gb/s was successfully demonstrated using test equipment for the CCF. Therefore, the proposed CCF shows promise for possible use in next-generation broadband fiber amplifier applications. The remainder of this paper is organized as follows: Section II describes the fabrication process of the CCFs, followed by the measurement and results in Section III. A discussion and conclusion are presented in Section IV.

II. FABRICATION

The gain of the CCF is related to the Cr^{4+}-ions concentrations in the Cr:YAG chromium oxide (Cr_2O_3) and calcium oxide (CaO) on the surface of the Cr:YAG rods, followed by an annealing process, was found effective in increasing the concentration of Cr^{4+}-ions [15], [16], [17], [18]. We used an electron-beam evaporator to coat a brown Cr_2O_3/CaO film on bulk 300-μm Cr:YAG rods. When the Cr diffuses internal to the Cr:YAG fiber, the ions are Cr^{2+}, Cr^{3+} and Cr^{4+} [16]. The coating of the CaO on the outer layer of Cr_2O_3 increases the content of Cr^{4+}-ions through charge compensation with Cr^{3+} by divalent ions of Ca^{2+} [13]. Introducing the Ca^{2+} by dielectric coating is a suitable choice in the Cr:YAG rod since Ca^{2+} has a better lattice matching then other divalent ions. Besides, the addition coating of CaO layer on the outer layer of Cr_2O_3 layer prevents out-diffusion of Cr-ions from the core [12]. The Cr^{4+}(tetra) enhanced mechanism of annealing process of chemical shifts might be represented by the two equations as follow [10]:

$$Cr^{3+}\,(\text{octa}) + 1/2\ O_2 \rightleftharpoons Cr^{4+}\,(\text{octa}) + O^{2-} \tag{1}$$

$$Cr^{4+}\,(\text{octa}) + Al^{3+}\,(\text{tetra}) \rightleftharpoons Cr^{4+}\,(\text{tetra}) + Al^{3+}(\text{octa}) \tag{2}$$

Equations (1) and (2) showed that the Cr^{3+}(octa) in the Cr:YAG adsorbed oxygen and transformed into the Cr^{4+}(octa) and then the Cr^{4+}(octa) transformed into the Cr^{4+}(tetra), resulting in the higher fluorescence intensity.

The dielectric coated 300-μm diameter Cr:YAG rod was regrown by LHPG to reduce its diameter to 80-μm and then to 19-25 μm for the Cr:YAG fiber. Fig. 1 shows a growth system of the LHPG which consists of a continuous-wave CO_2 laser with 4.4-mm beam diameter and less than $\pm$0.4% power fluctuation, an adjustable expander, two CCDs, and a growth chamber [8]. In order to fabricate smaller fiber core and longer fiber with good uniformity, a novel predictive control was employed [12]. All factors influencing laser power, such as operating current, laser mode distribution, heat dissipation, should be controlled to ensure stability of operation. In this study, we adjust the duty cycle of CO_2 laser by employing a predictive control for plain input current signal stabilization, which consists in controlling the power ripple of CO_2 laser fluctuations within $\pm$ 0.1% to reduce power gap during LHPG process. The fiber growth rates and molten zone sizes for the small core diameter was less than 0.29 cm/min and 16-μm, respectively. Therefore, we are able to constantly maintain the conical molten zone in fiber growth for small fiber-core fabrication. The CCF is the crystal fiber and cannot be curved to more than 1-meter radius of curvature.

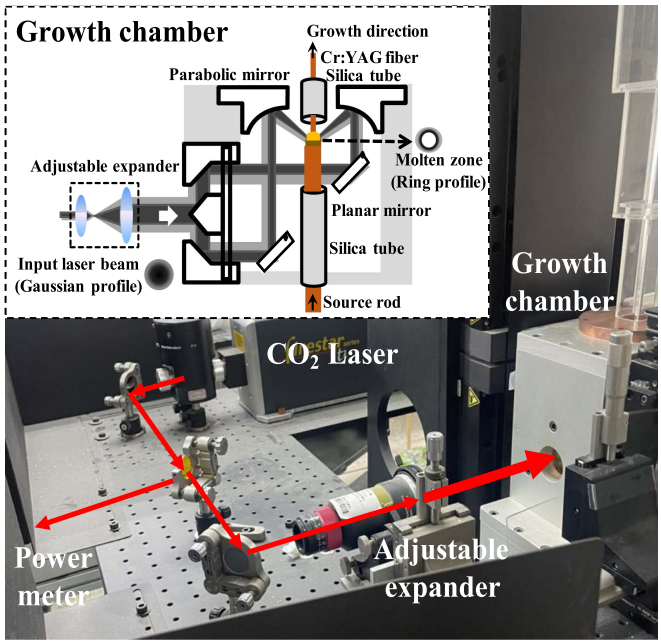

Fig. 1. The structure of LHPG system and growth chamber.

After the LHPG process, a thermal annealing technique was adopted. The annealing temperature was about 1000 °C for an annealing time of 12 hours. We choose the high-index glass ($n_{cladding} = 1.8275$) as the fiber cladding to match up with the Cr:YAG ($n_{core} = 1.8280$) as the core material. In order to verify the single-mode characteristics of the 19-, 20-, and 25-μm core of CCFs, we have measured the near-field and far-field patterns with 1550-nm wavelength. For single mode characteristics, the relationship between the divergence angle of far-field and the mode field diameter (MFD) of near field is given by [19]:

$$\text{Divergence angle}_{(\text{Single mode})} = 2\lambda/(\text{MFD} * \pi) \tag{3}$$

We have measured both the near and the far field of the CCF, as shown in Figs. 2 to 4. Figs. 2 and 3 show the schematic of far-field and near-field pattern measurement and the CCD

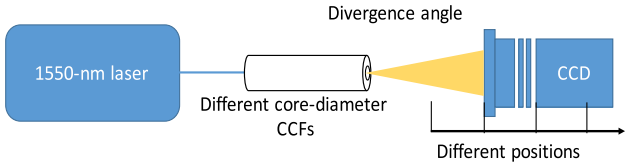

Fig. 2. Structure of far-field pattern measurement.

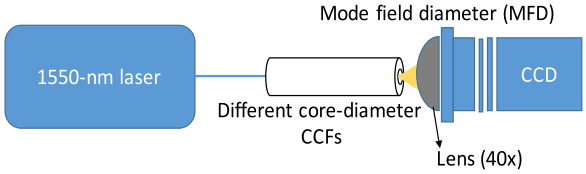

Fig. 3. Structure of near-field pattern measurement and where the 40x lens provides a x5 magnification of the near field distribution on the CCD.

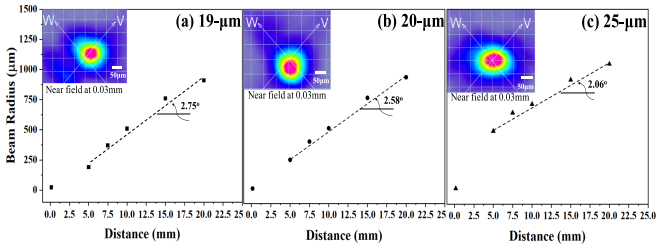

Fig. 4. Beam radius as function of distance for near-field MFD and far-field of divergence angle for different core diameters of (a) 19-, (b) 20-, and (c) 25-μm.

supplied the mode field distribution on which the MFD was measured, respectively. Fig. 4 shows the beam radius as function of distance for near-field of MFD (insert) and far-field of divergence angle for different core diameters. The near field distribution of modes showed near to circularly symmetrical. The divergence angle of 2.75°, 2.58°, and 2.06° were measured for the 19-, 20-, and 25-μm core of the CCFs, respectively, these values are to be compared to theoretical values of 2.76°, 2.58°, and 2.06° coming from (3). The MFD of 20.5-, 21.9-, 27.4-μm at 1.55-μm wavelength for the 19-, 20-, and 25-μm core of the CCFs, respectively, were measured by the near-field patterns. Based on reference [19], these measured date of the MFDs and divergence angles were satisfied the (3) for the single mode characteristics of the CCFs.

Recent studies have reported on Cr^{4+} enhancement in CCFs using polarization pumping techniques [12]. Three classes of sites oriented along the crystallographic axes are labeled X:(010), Y:(100), and Z:(001), and their respective Z-axes are parallel to the crystallographic axes of the host Cr^{4+}-ion. The cross-section of ground-state absorption with a pump beam polarized along the (001) axis is larger than with a pump beam polarized orthogonal to the (001) axis. Therefore, when the polarization of the pump and the signal are parallel to the same crystal axis, the CCF amplifier has the best performance [20].

Finally, four different types of CCF are listed in Table II. To assess the quality of growth, we used the standard deviation of the core diameter as a parameter. A smaller standard deviation

TABLE II
FOUR DIFFERENT FABRICATION PARAMETERS OF THE CCFS

Fiber index	A	B	C	D
Rod diameter (μm)	80	80	80	80
Fiber growth rate (cm/min)	0.29	0.22	0.17	0.14
Molten zone size (μm)	16	16	13	12
Core diameter (μm)	25	25	20	19
Cladding diameter (μm)	300	300	300	300
Fiber length (cm)	24	34	8	18
Core diameter standard deviation (μm)	0.25	0.32	0.60	0.60
Annealing (°C)	NA	1000 12 hrs	1000 12 hrs	1000 12 hrs
Cr_2O_3/CaO film coating (nm)	NA	Cr_2O_3:900 CaO:4500	Cr_2O_3:560 CaO:2800	Cr_2O_3:560 CaO:2800

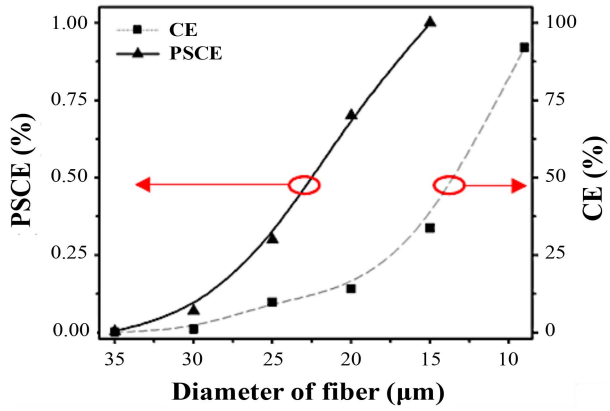

Fig. 5. The measured coupling efficiency (CE) and pump-to-signal-conversion efficiency (PSCE) of Cr:YAG fibers.

indicates better growth quality for the CCFs in the LHPG process. This leads to a better light path, reduces losses, and results in higher fluorescence intensity and gain. A standard deviation below 0.6-μm was set as a limit to indicate good growth quality of the CCFs in the LHPG process [12].

III. MEASUREMENTS AND RESULTS

Because of the coupling mode-mismatch from different core diameter size between CCF and single-mode fiber, we used an accurate control with a precise conical molten-zone shape in growth process to fabricate smaller core of 19-μm and reduce the coupling mode-mismatch effect, leading to a higher coupling efficiency (CE) and the PSCE, which defined as the ratio of output signal power to input pump power. The different core diameters of CCF were butted coupling with a single-mode fiber by a mechanical splicer, respectively, to measure the power rate between input and output power. In order to avoid reflections due to a small gap between fibers, we used the index-matching fluid between the CCF and single-mode fiber. Fig. 5 shows the setup for the measurement of CE and PSCE of CCFs of different core diameters. The PSCEs of the samples B, C

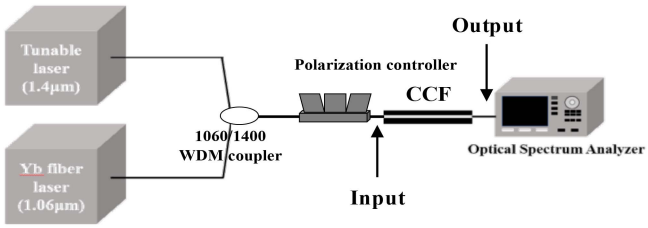

Fig. 6. Structure of gain measurement.

and D were 0.3, 0.7, and 0.8%, respectively. The CEs of the samples B, C, and D were 10%, 20%, and 25%, respectively. The result showed that the CE significantly improved as fiber diameter reduced. In comparison with the 25-μm core CCF, the CE and PSCE of the 19-μm core CCF are increased by 2.5 and 2.7 times, respectively. The internal power conversion efficiency of the CCF strongly depends on the core diameter between single mode fiber of 9-μm core diameter and the CCF. A 9-μm core diameter of the CCF is currently under development. Therefore, the coupling mode-mismatch between CCF and single-mode fiber may be solved to significant improvement the internal power conversion efficiency of the CCF. In Fig. 5, the 9-μm and 15-μm core CCFs had been fabricated. However, the length of these two fibers were too short to measure net gain.

The system gain of fiber amplifier is expressed as the ratio between the output signal and the input signal amplitude [21]. Net gain is the system gain plus total loss, which is contributed by the coupling loss, the scattering and absorption losses, the excited sate absorption, and other loss effects of the CCF. A 1060-nm Nd:YAG laser pump source, a 1400-nm signal source with 0.3-mW output power, and a polarization controller were used for the measurement, as shown in Fig. 6. The result of the optical amplification of the CCF signal was detected by an optical spectrum analyzer (Anritsu MS9740A). Then, the total loss of the CCF was measured by the cutback method with no pump power. An CCF was spliced with a single mode fiber by a mechanical splicer for transmission loss measurement. The total loss was measured 0.23 dB/cm at 1400-nm.

Fig. 7 shows the measured net gain as a function of pumping power of the CCFs for different core diameters of 19, 20, 25, and 25 μm, and fiber lengths of 18, 8, 34, 24 cm, with different coating and annealing conditions at a wavelength of 1400-nm, as listed in Table III. The net gains of 6.4-dB [8] and 11-dB [12] on the 24 and 34 cm lengths of the samples A and B were measured with and without coating and annealing, respectively. In comparison to the samples B and D, the 55% (a) - (b) Sample B with BTB and pump 500 mW, respectively (c) - (d) Sample C with BTB and pump 500 mW, respectively (e) - (f) Sample D with BTB and pump 500 mW, respectively net gain improvement was mainly achieved by further CE and PSCE improvement. This result confirms that optimization of the Cr^{4+} concentrations for the CCFs by small core diameter, which provides the significant gain improvement. The noise figure (NF) of fiber amplifiers is defined as the noise factor in dB, NF = 10 log (SNR_{in} / SNR_{out}), where

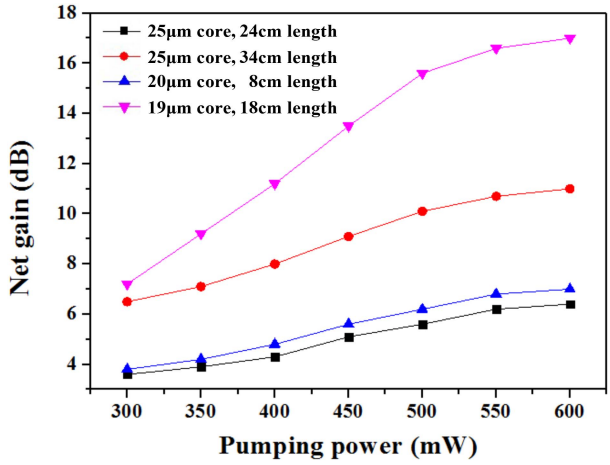

Fig. 7. Net gain as a function of pumping power of CCFs.

TABLE III
EFFECTS PROVIDED BY DIFFERENT TREATMENT CONDITIONS

Fiber index	A	B	C	D
Core diameter (μm)	25	25	20	19
Fiber length (cm)	24	34	8	18
Coating layer (nm)	No	Cr_2O_3:900 CaO:4500	Cr_2O_3:560 CaO:2800	Cr_2O_3:560 CaO:2800
Thermal annealing	No	Yes	Yes	Yes
Polarization pumping	No	Yes	Yes	Yes
Net gain (dB)	6.4	11	7	17
Gain-Per-Unit-Length Efficiency (dB/m)	27	32	88	94
Noise figure (dB) at pump power (mW)	NA	10.3 500	5.9 500	4.2 500
Eye diagram	NA	Clear	Clear	Clear
Bit error rate (NA)	NA	1.0×10^{-8}	6.1×10^{-9}	2.0×10^{-9}

the SNR_{in} and SNR_{out} are the input and output signal-to-noise ratios, respectively [21]. For the NF measurement, we used the same setup like for the gain measurement and added a digital serial analyzer (Tektronix DSA8300), measuring the input and the output optical powers, converted to electrical signals by a photodetector, and the resulting the signal-to-noise ratios of the CCF.

Fig. 8 shows the measured NF as a function of pumping power of the CCFs for different core diameters of 19, 20, and 25 μm with input signal power of 0.3 mW, as listed in Table III. The measured noise figures were from 4.2-dB to 10.3-dB for different core diameter of CCFs. The noise figure of Table III clearly showed that the smaller core of 19-μm exhibits a 4.2-dB lower noise figure than the larger core of 25-μm. In optical communication systems, there is a trade-off relationship between the fiber gain and noise figure of the fiber amplifier. Typically, when the gain of the optical amplifier is higher, its noise figure is also higher.

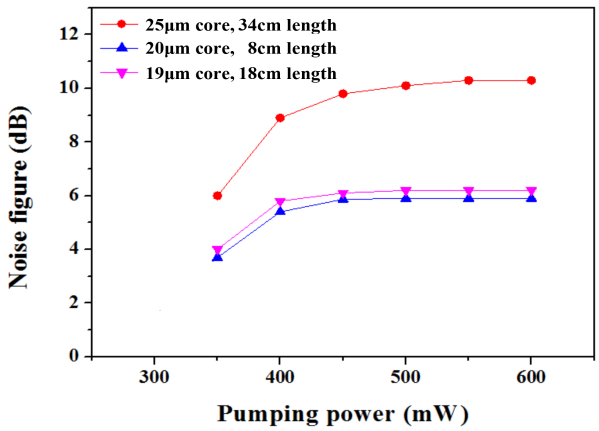

Fig. 8. Noise figure as a function of pumping power of CCFs.

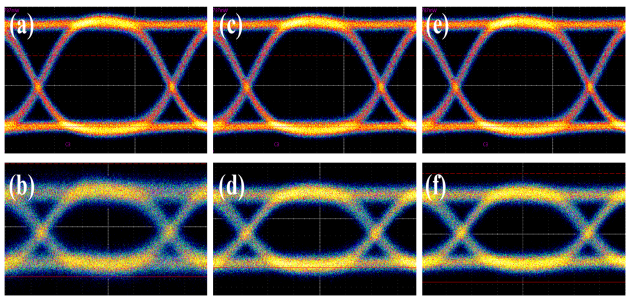

Fig. 9. The measured eye diagrams of different CCFs. (a), (b) Sample B with BTB and pump 500 mW, respectively. (c), (d) Sample C with BTB and pump 500 mW, respectively. (e), (f) Sample D with BTB and pump 500 mW, respectively.

In order to characterize the performance of CCFs in fiber transmission, a 10-Gb/s data rate with bit-error rate (BER) testing system is employed to investigate the performance of long-haul optical fiber transmission over 10-km with an attenuation of 1.8-dB. A 1400 nm signal transmitter optical sub-assembly (TOSA) and a 1064 nm pumping source were adopted in the measurement. A non-return-to-zero (NRZ) electrical 10-Gb/s pseudo random binary sequence with pattern length of 2^{31}-1 was generated by pulse pattern generator sending into a Mach-Zenhder modulator and then creating 10-Gb/s optical data. After receiving from a high-speed photo-detector to convert electrical signal, eye diagram and BER were obtained from a sampling oscilloscope with an electrical bandwidth of 10 GHz and error detector system. Eye diagram was constructed by generating a pseudorandom pattern of zeros and ones at a uniform rate but at a random fashion. When such pulses are superimposed upon each other simultaneously an eye pattern will be formed. The measured BER with different core diameter of CCFs at pumping 500-mW were 1.0×10^{-8}, 6.1×10^{-9}, and 2.0×10^{-9} for samples B, C, and D, respectively, as listed in Table III. These results showed the clear eye openings without waveform distortion in these eye patterns, as shown in Fig. 9.

IV. Conclusion

In summary, we have demonstrated a record net gain of 17-dB in a 19-μm fiber core for 300-nm broadband CCFs employing LHPG and Cr^{4+} optimization. The gain-per-unit- length of the CCF was about 94 dB/m, which was higher than the currently achieved Er and Bi-doped fibers of 0.6–3 dB/m [4], [7]. A novel accurate control to constantly maintain conical molten-zone shape in the LHPG process was proposed to fabricate a small fiber core of 19-μm. The Cr^{4+} concentrations optimization of the Cr:YAG was obtained by a thicker dielectric coating, thermal annealing, and polarization pumping were measured. The Cr^{4+}-ions optimization was the divalent cation of Ca^{2+} evaluation for the charge compensator in the Cr:YAG to increase the Cr^{4+} during coating [12], [13], and Cr^{4+}(tetra)-ions concentration recovery from the Cr^{3+}(octa) -ions in the Cr:YAG fiber during annealing [14], [15]. With an optical-fiber system testing of the CCF, a 10-Gb/s data rate with BER testing system was displayed by realizing the fiber transmission of signal with gain through the CCFs.

This breakthrough in the CCF technology could have far-reaching implications in a variety of industries, from telecommunications to sensing and medical devices. The achievement in fabrication of CCFs with high Cr^{4+} fluorescence makes it possible to develop the CCF as a broadband light source for ultrahigh resolution optical coherence tomography (OCT) and ultrafast mode-locked fiber laser. By enabling higher gains and better signal-to-noise ratios, the CCFs may revolutionize the way we communicate and gather information. With continued research and development, the CCFs may prove to be a valuable tool for advancing technology used in the next-generation broadband fiber amplifiers.

References

[1] T. Kasamatsu, Y. Yano, and H. Sekita, "1.50-μm-band gain-shifted thulium- doped fiber amplifier with 1.05- and 1.56-μm dual-wavelength pumping," *Opt. Lett.*, vol. 24, no. 23, pp. 1684–1686, Dec. 1999.

[2] S. V. Firstov et al., "Wideband bismuth- and erbium-codoped optical fiber amplifier for C + L + U-telecommunication band," *Laser Phys. Lett.*, vol. 14, Oct. 2017, Art. no. 110001.

[3] H. K. Dan et al., "Effects of Y^{3+}on the enhancement NIR emission of Bi^{+}-Er^{3+} co-doped in transparent silicate glass-ceramics for Erbium-doped fiber amplifier (EDFA)," *J. Lumin.*, vol. 219, Mar. 2020, Art. no. 116942.

[4] N. A. A. Ramlan, R. Zakaria, N. F. Zulkifli, N. Kasim, R. A. M. Yusoff, and A. A. A. Jafry, "Indium Selenide as passive saturable absorber for Q-switching in Erbium-doped fiber lasers," *Opt. Fiber Technol.*, vol. 72, Jul. 2022, Art. no. 102922.

[5] N. Aryapriya et al., "Concentration-Dependent fluorescence and judd–ofelt analysis of trivalent-praseodymium-doped alkali fluoroborate glass," *J. Electron. Mater.*, vol. 49, no. 6, pp. 3624–3633, Mar. 2020.

[6] Y. Ohishi, T. Kanamori, T. Kitagawa, S. Takahashi, E. Snitzer, and G. H. Sigel, "Pr3+ -doped fluoride fiber amplifier operating at 1.31 μm," *Opt. Lett.*, vol. 16, no. 22, pp. 1747–1749, Nov. 1991.

[7] Y. Wang, N. K. Thipparapu, D. J. Richardson, and J. K. Sahu, "High gain Bi-doped fiber amplifier operating in the E-band with a 3-dB bandwidth of 40nm," in *Proc. Opt. Fiber Commun. Conf. Exhib.*, 2021, pp. 1–3.

[8] C. N. Liu, T. H. Wang, T. S. Rou, N. K. Chen, S. L. Huang, and W. H. Cheng, "Higher gain of single-mode Cr-doped fibers employing optimized molten-zone growth," *J. Lightw. Technol.*, vol. 35, no. 22, pp. 4930–4936, Nov. 2017.

[9] C.- N. Liu, J.- W. Li, C.- C. Yang, C. Tu, and W.- H. Cheng, "Higher-gain of broadband single-mode chromium-doped fiber amplifiers by tetrahedral-chromium enhancement," in *Proc. Opt. Fiber Commun. Conf. Exhib.*, 2019, pp. 1–3.

[10] C. N. Liu et al., "Enhancement of tetrahedral chromium (Cr^{4+}) concentration for high-gain in single-mode crystalline core fibers," *IEEE Photon. J.*, vol. 12, no. 2, Apr. 2020, Art. no. 7200821.

[11] C. N. Liu, J. W. Li, C. C. Yang, C. Tu, and W. H. Cheng, "Tetrahedral-Cr enhancement employing dielectric coating for higher gain of broadband Cr-doped fiber amplifiers," in *Proc. Opt. Fiber Commun. Conf. Exhib.*, 2020, pp. 1–3.

[12] C. N. Liu, C. M. Liu, S. L. Huang, and W. H. Cheng, "Broadband single-mode Cr-doped crystalline core fiber with record 11-dB net gain by precise laser-heated pedestal growth and tetrahedral chromium o broadband fiber amplifier optimization," *J. Lightw. Technol.*, vol. 39, no. 11, pp. 3531–3538, Jun. 2021.

[13] P. Y. Chen, C. L. Chang, K. Y. Huang, C. W. Lan, W. H. Cheng, and S. L. Huang, "Experiment and simulation on interface shapes of an yttrium aluminum garnet miniature molten zone formed using the laser-heated pedestal growth method for single-crystal fibers," *J. Appl. Crystallogr.*, vol. 42, pp. 553–563, May 2009.

[14] C. Y. Lo and P. Y. Chen, "Three-dimensional simulation and experiment on micro-floating zone of LHPG with asymmetrical perturbation," *J. Cryst. Growth*, vol. 362, pp. 45–51, Jan. 2013.

[15] S. A. Markgraf, M. F. Pangborn, and R. Dieckmann, "Influence of different divalent co-dopants on the Cr^{4+} of Cr-doped $Y_3Al_5O_{12}$ content," *J. Cryst. Growth*, vol. 180, no. 1, pp. 81–84, Sep. 1997.

[16] C. Koepke, K. Wisniewski, and M. Grinberg, "Excited state spectroscopy of chromium ions in various valence states in glass," *J. Alloys Compounds*, vol. 341, no. 1-2, pp. 19–27, Jul. 2002.

[17] R. Feldman, Y. Shimony, and Z. Burshtein, "Dynamics of chromium ion valence transformations in Cr, Ca:YAG crystals used as laser gain and passive Q-switching media," *Opt. Mater.*, vol. 24, no. 1-2, pp. 333–344, Nov. 2003.

[18] A. Sugimoto, Y. Nobe, and K. Yamagishi, "Crystal growth and optical characterization of Cr, Ca: Y3Al5O12," *J. Cryst. Growth*, vol. 140, no. 3-4, pp. 349–354, May 2008.

[19] A. M. Kowalevicz, Jr. and F. Bucholtz, "Beam divergence from an SMF-28 optical fiber," *J. Phys. Sci.*, vol. 9, pp. 635–648, 2006.

[20] V. Kartazaev and R. R. Alfano, "Polarization influence of excited state absorption on the performance of Cr^{4+}:YAG laser," *Opt. Commun.*, vol. 242, pp. 605–611, Dec. 2004.

[21] P. C. Becker, N. A. Olsson, and J. R. Simpson, "Erbium-doped fiber amplifiers: Fundamentals and technology," in *Optics and Photontheics*, 1st ed., P. L. Kelly, Ed. Cambridge, MA, USA: Academic, 1999, pp. 251–253.

[22] M. Movassaghi, M. K. Jackson, V. M. Smith, and W. J. Hallam, "Noise figure of erbium-doped fiber amplifiers in saturated operation," *J. Lightw. Technol.*, vol. 16, no. 5, pp. 812–817, May 1998.

[23] K. S. Abedin et al., "Amplification and noise properties of an erbium-doped multicore fiber amplifier," *Opt. Exp.*, vol. 19, no. 17, pp. 16715–16721, Aug. 2011.

[24] S. M. Yeh et al., "Mode matching and insertion loss in ultra-broadband Cr-doped multimode fibers," *Opt. Lett.*, vol. 33, no. 8, pp. 785–787, Apr. 2008.